

Inverting Specular Neutron Reflectivity From Symmetric, Compactly-Supported Potentials

N. F. Berk and C. F. Majkrzak

*Materials Science and Engineering Laboratory, National Institute of Standards and Technology,
 Gaithersburg, MD 20899, U.S.A.*

(Received 12 February 1996; accepted 1 May 1996)

A method is described for inverting specular neutron reflectivities from real, symmetric, compactly-supported potentials of known thickness. For such potentials, the phase of the complex reflection coefficient is equal to the phase of the transmission coefficient plus a known phase shift and thus can be retrieved from a single measurement of reflectivity using a logarithmic dispersion relation for the transmission. The resulting reflection coefficient can be inverted to find the potential by solving the Gel'fand-Levitan-Marchenko integral equation. The method is general, to the extent that symmetric potentials can be formed by abutting two identical specimens of a film of interest.

KEYWORDS: neutrons, specular reflection, phase determination, inversion,
 symmetric potentials, Gel'fand-Levitan-Marchenko equation

§.1. Introduction

Recent progress has been made in the problem of measuring the phase of neutron reflectivity, thereby opening new possibilities for the analysis of specular reflectometry, including the determination of scattering length densities by direct inversion of data. These new theoretical methods of phase determination are effectively restricted to neutrons because of an express requirement that the scattering length density be real valued, which is well met for neutrons in most cases but not for x-rays.

In one approach,^{1,2)} both the complex reflection coefficient and its norm, the measured reflectivity, are shown to be expressed by the same three functions of the elements of a 2×2 transfer matrix. These functions are measurable from the reflectivity spectra of three samples, each consisting of the same unknown film and one of three known reference layers. While this method requires three measurements, it entails only algebraic and local extraction of the reflection amplitude, the phase determination at each wavevector depending only on data at that point.

Another method, introduced here, requires only a single spectrum but is restricted to mirror symmetric films, i.e., films which present the same scattering length density profile from either direction, and it does entail non-local transformation of the data.

Knowledge of the complex reflection coefficient enables direct inversion of neutron reflectometry using the Gel'fand-Levitan-Marchenko (GLM) integral equation or related methods.³⁻⁶⁾

We lay general groundwork in Sec.2 and specialize to the case of mirror symmetry in Sec.3. The GLM equation is discussed in Sec.4 with a model application.

§.2. Formalism: the Transfer Matrix

The theory of specular reflectivity from a film can be cast as the problem of solving a 1-dimensional Schrödinger equation for the variation of the wave

function along the direction normal to the surface, conventionally taken as the z -axis:

$$-\frac{d^2\psi(k_z, z)}{dz^2} + q(z)\psi(k_z, z) = k_z^2\psi(k_z, z) \quad (1)$$

where

$$q(z) = 4\pi\rho(z) \quad (2)$$

and where $\rho(z)$ is the neutron scattering length density. The wavevector k_z is the z -component of the incident wavevector. In the most general case, the potential $q(z)$ may be supported on the whole z -line, but here we consider only the more restrictive, but still very useful, case of potentials having compact support on $0 \leq z \leq L$; i.e., $q(z)=0$ for $z<0$ and $z>L$, where L is the thickness of the film, which we will assume is known. The subsequent formulation also assumes that the film is freely supported, i.e., that the fronting and backing media are vacuum. Finally, we take $q(z)$ to be real-valued, which usually is a very good approximation for neutrons. In Sec.3 we will make further restrictions to mirror-symmetric and non-negative potentials. Thus, for the potentials of concern, the physical solution of Eq.(1) has canonical forms outside the support of $q(z)$, namely,

$$\psi(k_z, z) = e^{ik_z z} + r(k_z)e^{-ik_z z}, \quad z < 0, \quad (3a)$$

and

$$\psi(k_z, z) = t(k_z)e^{ik_z z}, \quad z > L, \quad (3b)$$

where $r(k_z)$ and $t(k_z)$ are the complex reflection and transmission coefficients, respectively. The measured reflectivity is $|r(k_z)|^2$. Among the several means of solution methods available for Eq. (1) in $[0, L]$ we use the transfer matrix method, which proves to be a particularly convenient analytical tool for our purposes.

The transfer matrix^{7,8)} is a 2×2 matrix which gives a concise connection between the disjoint solutions in Eq.(3). The requirements of continuity of $\psi(k_z, z)$ and $\psi'(k_z, z)$ at $z = 0$ and at $z = L$ provide a determination of $r(k_z)$ and $t(k_z)$ in terms of the four elements of the transfer matrix, by analogy to the effect of the boundary conditions across a single interface. Thus for $0 \leq z \leq L$, let

$$\chi(k_z, z) = \mathbf{M}(k_z, z)\chi(k_z, 0), \quad (4)$$

where

$$\chi(k_z, z) = \begin{pmatrix} \psi(k_z, z) \\ k_z^{-1}\psi'(k_z, z) \end{pmatrix}, \quad (5)$$

and

$$\mathbf{M}(k_z, z) = \begin{pmatrix} A(k_z, z) & B(k_z, z) \\ C(k_z, z) & D(k_z, z) \end{pmatrix} \quad (6)$$

is the transfer matrix. Consistency at $z=0$ demands

$$\mathbf{M}(k_z, 0) = \mathbf{1} \quad (7)$$

The evolution of $\mathbf{M}(k_z, z)$ is obtained by differentiating Eq.(5) and using Eq.(1), which leads to

$$\frac{d\mathbf{M}(k_z, z)}{dz} = \Gamma(k_z, z)\mathbf{M}(k_z, z), \quad (8)$$

where

$$\Gamma(k_z, z) = \begin{pmatrix} 0 & k_z \\ k_z^{-1}q(z) - k_z & 0 \end{pmatrix}. \quad (9)$$

The solution of Eq.(8) is unique, subject to the initial value, Eq.(7).

For real-valued potentials, $\mathbf{M}(k_z, z)$ is real for all real k_z . Also, $\mathbf{M}(k_z, z)$ is unimodular, i.e.,

$$AD - BC = 1 \quad (10)$$

To derive this, differentiate $AD-CD$ with respect to z , then use Eqs.(8) and (7).

Substitution of Eq.(3) into Eq.(4) gives two equations for $r(k_z)$ and $t(k_z)$, which have solutions

$$r = \frac{B + C + i(D - A)}{B - C + i(D + A)}, \quad (11a)$$

and

$$t = \frac{2ie^{-ik_z L}}{B - C + i(D + A)}, \quad (11b)$$

and where it can be confirmed that $|r|^2 + |t|^2 = 1$. Since \mathbf{M} is real, the complex natures of r and t are made explicit by Eq.(11). We also note for later use that

$$\mathbf{M}(-k_z, z) = \begin{pmatrix} A(k_z, z) & -B(k_z, z) \\ -C(k_z, z) & D(k_z, z) \end{pmatrix}, \quad (12)$$

which follows from Eq.(4), and thus from Eq.(11), that

$$r(-k_z) = r^*(k_z), \quad (13a)$$

and

$$t(-k_z) = t^*(k_z). \quad (13b)$$

§.3. Determining Phase for Symmetric Potentials

For mirror-symmetric potentials, which satisfy $q(z) = q(L-z)$, it can be shown that⁹⁾

$$D(k_z, L) = A(k_z, L) \quad (14)$$

thus

$$\hat{r} = \frac{B + C}{B - C + 2iA}, \quad (15a)$$

and

$$\hat{t} = \frac{2ie^{-ik_z L}}{B - C + 2iA}, \quad (15b)$$

where ($\hat{}$) signifies this special case of r and t . Now

$$\frac{\hat{r}}{\hat{t}} = \frac{B + C}{2i} e^{ik_z L} = \frac{|\hat{r}|}{|\hat{t}|} e^{i(\hat{\phi}_r - \hat{\phi}_t)}. \quad (16)$$

Thus

$$e^{i(\hat{\phi}_r - \hat{\phi}_t) - k_z L} = \frac{\sqrt{1 - |\hat{r}|^2}}{2i|\hat{r}|} (B + C). \quad (17)$$

With the help of Eq.(10) it can be shown that^{1,10)}

$$2 \frac{1 + |\hat{r}|^2}{1 - |\hat{r}|^2} = B^2 + C^2 + 2A^2, \quad (18)$$

so that, again using Eq.(10),

$$B + C = \frac{\pm 2|\hat{r}|}{\sqrt{1 - |\hat{r}|^2}}. \quad (19)$$

Therefore, from Eq.(17),

$$e^{i(\hat{\phi}_r - \hat{\phi}_t - k_z L)} = \pm i. \quad (20)$$

Before going to the next step, it is useful to have the limiting behaviors of $\mathbf{M}(k_z, z)$ as $k_z \rightarrow 0$ and $k_z \rightarrow \infty$. It can be shown from Eq.(8) that

$$\lim_{k_z \rightarrow 0} \mathbf{M}(k_z, L) = \begin{pmatrix} O(1) & O(k_z) \\ O(k_z^{-1}) & O(1) \end{pmatrix}; \quad (21)$$

i.e., $A \rightarrow O(1)$, $D \rightarrow O(1)$, $B \rightarrow 0$, and $C \rightarrow \infty$. Here $O(1) = O(k_z^0)$ means a finite value, independent of k_z . Also,

$$\lim_{k_z \rightarrow 0} \mathbf{M}(k_z, L) = \begin{pmatrix} \cos(k_z L) & \sin(k_z L) \\ -\sin(k_z L) & \cos(k_z L) \end{pmatrix}; \quad (22)$$

i.e., $A \rightarrow D \rightarrow \cos(k_z L)$, and $B \rightarrow -C \rightarrow \sin(k_z L)$. In particular, since $C(k_z, L) \rightarrow \infty$ as $k_z \rightarrow 0$, it follows that

$$\lim_{k_z \rightarrow 0} r(k_z) = -1, \quad (23a)$$

and

$$\lim_{k_z \rightarrow 0} t(k_z) = -iO(k_z), \quad (23b)$$

and thus we may define

$$\phi_r(0) = -\pi \quad (24a)$$

and

$$\phi_t(0) = -\pi/2. \quad (24b)$$

These limits are quite general for real, compactly-supported potentials. Therefore from Eq.(20) and Eq.(24) we have in the present case,

$$\hat{\phi}_r(k_z) = \hat{\phi}_t(k_z) - \frac{\pi}{2} + k_z L, \quad (25)$$

where we have chosen the branch of Eq.(20) which is consistent with Eq.(24). Also, whenever $\hat{r}(k_z)$ passes through the origin of the Argand diagram, i.e., the graph of the parametric curve $\hat{r}''(k_z)$ vs. $\hat{r}'(k_z)$, the phase angle decreases by π . Then Eq.(25) becomes

$$\hat{\phi}_r(k_z) = \hat{\phi}_t(k_z) - \frac{\pi}{2} + k_z L - n\pi, \quad (26)$$

for $k_n < k_z \leq k_{n+1}$, where $r(k_n) = 0$ for $n = 1, 2, \dots$; and where $n=0$ for $k_z \leq k_1$. In general, compactly-supported, symmetric potentials produce such zeros, where $k_n L \rightarrow n\pi$ as $n \rightarrow \infty$.¹¹⁾ Thus $\hat{\phi}_r(k_z)$ effectively lies within the interval $[-\pi/2, \pi/2]$ as $k_z \rightarrow \infty$.

The phase of $\hat{t}(k_z)$ is obtained from a logarithmic dispersion relation.¹²⁻¹⁴⁾ It is well-known that in the absence of bound states, $t(k_z)$ (and also $r(k_z)$) is analytic in the upper half k_z -plane.³⁻⁵⁾ Furthermore, from Eqs.(22),

$$\lim_{k_z \rightarrow \pm\infty} t(k_z) = \frac{2ie^{-ik_z L}}{2 \sin(k_z L) + 2i \cos(k_z L)} = 1. \quad (27)$$

It then follows from analytic continuation that

$$\lim_{|k_z| \rightarrow \infty} t(k_z) = 1 \quad (28)$$

for $\text{Im } k_z \geq 0$. Thus $\lim_{|k_z| \rightarrow \infty} \ln t(k_z) = 0$ in the upper half-plane. Moreover, one sees from Eq.(11b) that $t(k_z)$ has no zeros in the upper half plane, so that $\ln t(k_z)$ is finite for $\text{Im } k_z > 0$ and vanishes uniformly on the upper infinite semicircle. It follows¹⁵⁾ that $\ln t(k_z)$ satisfies a dispersion relation, which relates its imaginary part,

$\hat{\phi}_t(k_z)$, to the Hilbert transform of its real part, $\ln|t(k_z)| = \ln \sqrt{1 - |r(k_z)|^2}$; namely,

$$\phi_t(k_z) = -\frac{1}{\pi} \text{PP} \int_{-\infty}^{\infty} \frac{\ln \sqrt{1 - |r(k_z')|^2}}{k_z' - k_z} dk_z'. \quad (29)$$

Although $t(0)=0$, the resulting divergence in $\ln|t(k_z)|$ is integrable in Eq.(29). One notices that this result is

quite general for real, finite, non-negative compactly-supported $q(z)$, since such potentials can not have bound states, and they guarantee the "good" behavior needed for the dispersion relation. In particular, it also holds for our restriction to mirror-symmetric potentials, so that one may rewrite Eq.(29) with (\wedge) s.

Equations (26) and (29) comprise the algorithm for obtaining the phase of reflection from a reflectivity spectrum for the special but useful class of real, non-negative, compactly-supported potentials which are also mirror-symmetric, but which otherwise may have quite arbitrary shape. For computational purposes Eq.(29) may be rewritten as

$$\phi_t(k_z) = -\frac{k_z}{\pi} \text{PP} \int_0^{\infty} \frac{\ln(|t(k_z')|^2 / |t(k_z)|^2)}{k_z'^2 - k_z^2} dk_z'. \quad (30)$$

The relation in Eq.(26) is interesting, as well as useful. One sees from Eq.(27) that

$$\lim_{k_z \rightarrow \infty} \phi_t(k_z) = 0, \quad (31)$$

which may also be inferred from Eq.(29), since the numerator of the integrand is everywhere finite or integrable. Thus from Eq.(26),

$$\lim_{k_z \rightarrow \infty} \hat{\phi}_r(k_z) = -\frac{\pi}{2} + k_z L - n\pi. \quad (32)$$

Now it is well known that the limit of the scattering as $k_z \rightarrow \infty$ is given exactly by the Born approximation (BA). Thus Eqs.(26), (31), and (32) imply

$$\hat{\phi}_r(k_z) = \hat{\phi}_t(k_z) + \hat{\phi}_r^{BA}(k_z). \quad (33)$$

Indeed, in the Born approximation,

$$\begin{aligned} \hat{r}^{BA}(k_z) &= \frac{1}{2ik_z} \int_0^L e^{2ik_z z} q(z) dz \\ &= \frac{e^{2ik_z L}}{2ik_z} \int_0^L e^{-2ik_z z} q(z) dz \end{aligned} \quad (34)$$

for $q(z) = q(L-z)$. This can be written as

$$\hat{r}^{BA}(k_z) = e^{i(-\pi/2 + k_z L)} \hat{f}(k_z), \quad (35)$$

where $\hat{f}(k_z)$ is real, so that

$$\hat{\phi}_r^{BA}(k_z) = -\frac{\pi}{2} + k_z L - n\pi, \quad (36)$$

as in Eq.(33). Thus for mirror-symmetric potentials, the contribution to the phase of $\hat{r}(k_z)$ caused by dynamical scattering is entirely the phase of $\hat{t}(k_z)$.

§.4. Inverting the Reflection Spectrum

§.4.1. The GLM Equation

We have seen that for film potentials $q(z)$ of known thickness L which are non-negative and symmetric about $z = L/2$, the complex reflection coefficient $\hat{r}(k_z)$ can be

reconstructed from the reflectivity spectrum $|\hat{r}(k_z)|^2$; namely,

$$\hat{r}(k_z) = e^{i\hat{\phi}_r(k_z)} |\hat{r}(k_z)|, \quad (37)$$

where $\hat{\phi}_r(k_z)$ is determined from $|\hat{r}(k_z)|$; using Eqs.(26) and (30). Knowledge of $r(k_z)$ is sufficient to "invert" the spectrum, i.e., to determine $q(z)$ uniquely for potentials that do not support bound states and which are sufficiently regular, such as those having compact support. The prototype for formal inversion is the Gel'fand-Levitan-Marchenko (GLM) equation,³⁻⁵⁾ which for the case of real, non-negative, compactly-supported potentials, can be written as

$$K(z, y) + R(x + y) + \int_{-z}^z K(z, x)R(x + y)dx = 0, \quad (38)$$

for $y \leq z$. Here the "real space reflection coefficient" $R(z)$ is

$$R(z) = \int_{-\infty}^{\infty} r(k_z) e^{ik_z z} \frac{dk_z}{2\pi} = \text{Re} \int_0^{\infty} r(k_z) e^{ik_z z} \frac{dk_z}{\pi}, \quad (39)$$

where the second equality results from Eq.(13), so that $R(z)$ is real. The function $K(z, y)$ in the GLM equation is known as the Povzner-Levitan (PL) kernel⁵⁾ and satisfies $K(z, y)=0$ for $z \leq 0$, and for $-z \leq y < z$ when $z > 0$. Thus from Eq.(38),

$$R(z) = 0 \quad \text{for } z \leq 0, \quad (40)$$

which also follows from Eq.(39) and the analyticity of $r(k_z)$ in the upper half plane. Thus the GLM equation may be rewritten as

$$K(z, y) + R(x + y) + \int_0^{z+y} K(z, x - y)R(x)dx = 0. \quad (41)$$

The PL kernel¹⁶⁾ also has the remarkable property,³⁻⁵⁾

$$q(z) = 2 \frac{dK(z, z)}{dz}. \quad (42)$$

Thus $q(z)$ is known once the PL kernel is known. In our problem, then, the inversion of $|\hat{r}(k_z)|^2$ starts with the determination of $\hat{\phi}_r(k_z)$ using the algorithm of Sec.3 --the only step that depends on the restriction to symmetric potentials--proceeds to the computation of $R(z)$ using Eqs.(37) and (39), and culminates in the solution of the GLM equation for the PL kernel and the extraction of $q(z)$ by Eq.(42).

There is an interesting way of interpreting the latter part of this process. Recall from Eq.(34) that in the Born approximation

$$2ik_z r^{BA}(k_z) = \int_{-\infty}^{\infty} q(z) e^{2ik_z z} dz. \quad (43)$$

Taking the inverse Fourier transform of both sides leads to

$$-2 \frac{d}{dz} \int_{-\infty}^{\infty} r^{BA}(k_z) e^{-ik_z z} dk_z = \frac{1}{2} q\left(\frac{z}{2}\right), \quad (44)$$

and thus, comparing with Eq.(42), to

$$K(z, z) = -R^{BA}(2z). \quad (45)$$

That is, the diagonal of the exact PL kernel is the negative of the Born approximation to the real space reflection coefficient. One might say, therefore, that the function of solving the GLM equation for $K(z, y)$ is to "reduce" the exact real space reflection coefficient to the Born approximation, which is easily inverted for $q(z)$; in other words, the GLM equation effectively removes the dynamical scattering from $R(z)$. To go a bit further, set $y = z$ in Eq.(41) to get

$$K(z, z) + R(2z) + \int_0^{2z} K(z, x - z)R(x)dx = 0. \quad (46)$$

Then as $z \rightarrow 0$, the integral vanishes and

$$\lim_{z \rightarrow 0} R(2z) = -K(z, z) = R^{BA}(2z). \quad (47)$$

Thus the Born approximation is exact in a neighborhood of the leading edge of the potential.

§.4.2. A Solution Method

Much of the literature on solving the GLM and related equations deals with exploiting special assumptions about the analytic behavior of the real space reflection coefficient $R(z)$.¹⁷⁾ For the general case, numerical solution methods boil down to replacing the integral equation by a discrete matrix equation,¹⁸⁾ which we will not discuss, or to iteration on the "0-th" order solution

$$K^{(0)}(z, y) = -R(z + y), \quad (48)$$

which, as we have seen in Eq.(47), becomes exact as $y \rightarrow z$ and $z \rightarrow 0$ for potentials supported on $[0, L]$. In the next stage of iteration, one then would have

$$K^{(1)}(z, y) = -R(z + y) - \int_0^{z+y} R(z + x - y)R(x)dx, \quad (49)$$

and so on. We have found that this straightforward iteration scheme is well-adapted to implementation in symbolic mathematical software packages, such as are commercially available. One may take advantage of knowing the thickness L and the fact that $K(z, y)$ for $y \leq z$ and $z \leq L$ depends only on $R(x)$ for $0 \leq x \leq 2L$. We approximate the computed $R(x)$ in $[0, 2L]$ by an interpolating spline on N segments bounded by $N+1$ knots, $x_0=0, x_1, \dots, x_N=2L$; i.e.,

$$R(x) \rightarrow \sum_{n=1}^N R_n(x), \quad (50)$$

where

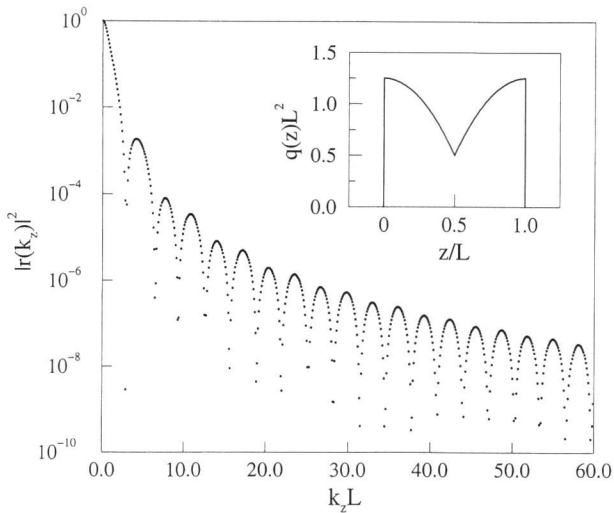


Fig.1. Simulated reflectivity spectrum (600 points) for model potential, shown in inset

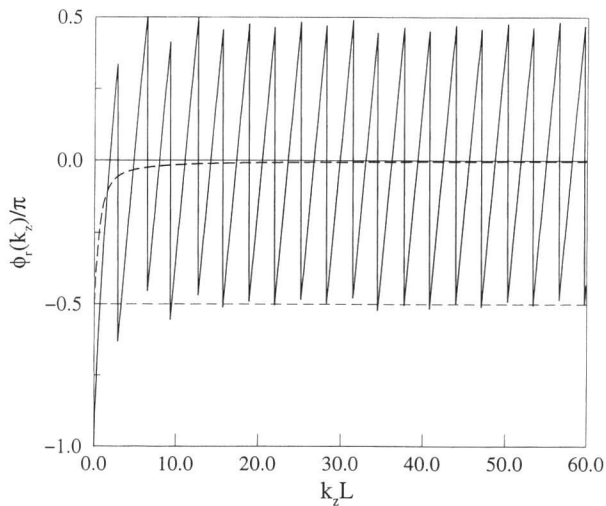


Fig.2. Computed phase of reflection (solid line); computed phase of transmission (dashed line).

$$R_n(x) = \begin{cases} \approx R(x), & (x_{n-1} \leq x < x_n) \\ 0, & (\text{otherwise}) \end{cases} \quad (51)$$

Taking Eq.(50) as an exact representation of $R(x)$ allows us to write the GLM equation as

$$K(z, y) = -R_n(z + y) - \sum_{m=1}^{n-1} \int_{x_{m-1}}^{x_m} K(z, x - y) R_m(x) dx + \int_{x_{n-1}}^{z+y} K(x, x - y) R_n(x) dx, \quad (52)$$

for $x_{n-1}/2 \leq z < x_n/2$. Thus when $n=1, 2, \dots, N$ in sequence, the second term on the *rhs* involves $K(z, x-y)$ on previously determined segments, and the unknown n -th segment appears only in the last integral. The form of Eq.(52) also requires $x_{n-1} \leq z+y < x_n$ and in the last term that $x_{n-1} \leq x < z+y$. Such constraints, although awkward in a numerical procedure, are transparent to a symbolic method when the segmental $R_n(x)$ are given as explicit polynomials. We need only iterate Eq.(52)

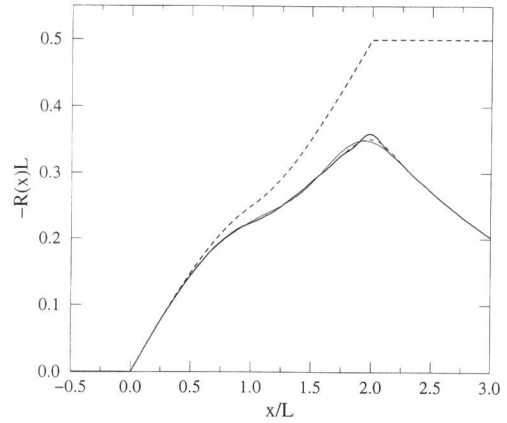


Fig.3. Computed real space reflection coefficient using 600 reflectivity points (heavy line); same using 300 points (light dash line) and for 200 points (light solid line); theoretical $K(x/2, x/2)$ (heavy dashed line).

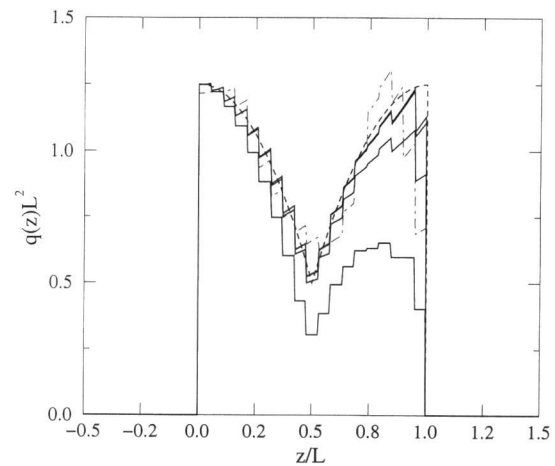


Fig.4. Potential from GLM equation. Results for 0, 1, 2, and 3 iterations are shown in order from bottom (heavy lines); model potential (heavy dashed line); result from data truncation at 200 points (light dashed line).

symbolically on $R_n(x)$ in the currently unknown segment; the resulting polynomial at each stage is available for all x, y , and z , and the required constraints can be applied at the end of the entire process for each segment to complete the chain:

$$R_n(x) \rightarrow K_n(z, y) \rightarrow K_n(z, z) \rightarrow q_n(z) \quad (53)$$

for $n = 1, 2, \dots, N$ in sequence.

There remains the question of choosing the degree of interpolating spline to approximate $R(x)$. Use of 0-degree splines, as in rectangular representations, gives discontinuous $R(x)$ and $K(z, z)$, and thus leads to undesirable singularities at the knots when Eq.(42) is applied. First-degree (linear) splines are continuous and lead to continuous $K(z, z)$, but the resulting $q(z)$ will display discontinuities at the knots. Higher degree splines lead to smoother representations of $q(z)$, but the concomitant overhead of symbolic computation increases rapidly, and high order interpolation can bring spurious structure into the approximation, which, in any case, need not be of better quality than the inference of $R(x)$ from the data. Linear interpolation seems a reasonable

compromise of competing concerns, and is easy to implement. In each segment we take

$$R_n(x) = a_n + b_n x, \quad (54)$$

where

$$a_n = \frac{x_n R(x_{n-1}) - x_{n-1} R(x_n)}{x_n - x_{n-1}}, \quad (55a)$$

and

$$b_n = \frac{R(x_n) - R(x_{n-1})}{x_n - x_{n-1}}. \quad (55b)$$

§.4.3. Example

We illustrate the method with the model potential drawn in the inset to Fig. 1, which on its support, $0 \leq z \leq L$, has the formula,

$$q(z)L^2 = 0.5 + \begin{cases} f(z/L + 1/2), & z \leq L/2, \\ f(z/L - 1/2), & z > L/2, \end{cases} \quad (56a)$$

where

$$f(x) = 3x(1-x). \quad (56b)$$

This potential is moderately strong, with $\bar{q}L^2 = 1$, where is the average value of $q(z)$ over $[0,L]$. The computed model reflectivity spectrum is shown in Fig.1, comprising 600 points with uniform spacing, $\Delta k_z L = 0.1$. The full range of data shown likely reaches the limits of instrumental feasibility for the foreseeable future. The spectrum was calculated using a standard technique of binning the potential on a fine scale and composing the transfer matrix as a product of transfer matrices for each bin.

These data were used to compute the reflection phase, $\phi_r(k_z)$, shown in Fig.2. First the transmission phase, $\phi_t(k_z)$, was computed from Eq.(30). Numerical integrations were done by a commercial mathematical package. The reflection phase then was composed from Eq.(26); the zeros of the spectrum were determined by visual inspection and were taken as the nearest tabulated $k_z L$ values.

The resulting real space reflection coefficient, $R(x)$, was computed from Eq.(39) using a commercial FFT algorithm. This is shown in Fig.3, along with $-R^{BA}(x)$, which is obtained directly from the model potential by integrating Eq.(44). The goal of solving the GLM equation is to "lift" the heavy line in the figure onto the dashed line, $-R^{BA}(x) = K(x/2, x/2)$.

Finally, the numerical solution of the GLM equation for $q(z)$ is shown in Fig.4. The input $R(x)$ was fit by an interpolating linear spline, as in Eq.(54). The x -interval $[0,2L]$ was divided into 19 uniform segments, determined---via the Fourier transform---by the effective real space resolution, $\Delta x = 2\pi/k_{z, max}$. The thick lines show the progression of the iterative process, starting with 0 iterations at the bottom; this is the potential that results if one assumes that $R(x) = R^{BA}(x)$. The process

effectively converges over $[0,L]$ after 3 iterations, shown at the top. Notice, however, that the solution essentially converges over the first half of the interval in 1 iteration. The jagged nature of the solution results from the polynomial representation within each segment, as discussed in Sec.4.2.

The figures also show results for truncation of the model data at $k_z L = 30$ (300 points) and $k_z L = 20$ (200 points). In Fig.4, these are determined on the same resolution as for the full data set, $k_z L = 60$, although lower resolution solutions would be appropriate for the smaller data sets. Actually, at this resolution the potentials determined from 600 and 300 points are nearly identical, and even the result using only 200 points is good over the first half of the support. Indeed, it is worth pointing out that since the otherwise unknown potential is known by construction to be symmetric,¹⁹⁾ its shape in fact is determined in the half-interval $[0, L/2]$; and this apparently can be ascertained reasonably well from a data set of achievable range and quality.

-
- 1) C.F. Majkrzak and N.F. Berk: *Phys. Rev. B* 15 (1995) 10827.
 - 2) V.O. deHaan, A.A. van Well, S. Adenwalla, and G.P. Felcher: *Phys. Rev. B* 15 (1995) 10830.
 - 3) K. Chadan and P.C. Sabatier: *Inverse Problems in Quantum Scattering Theory* (Springer-Verlag, New York, 1989).
 - 4) D.N. Ghosh Roy: *Methods of Inverse Scattering Problems in Physics* (CRC Press, Boca Raton, 1991).
 - 5) V.A. Marchenko: *Sturm-Liouville Operators and Applications* (Birkäuser Verlag, Boston, 1986).
 - 6) W. Rundell and P. Sachs: *SPIE Proceedings*, 1767 (1992) 31.
 - 7) P. Croce and B. Pardo: *Nouv. Rev. Opt. Appl.* 1 (1970) 229.
 - 8) S. Yamada, T. Ebisawa, N. Achiwa, T. Akiyoshi, and S. Okamoto: *Annu. Rep. Res. Reactor Inst. Kyoto Univ.* 11 (1978) 8.
 - 9) L.R. Clifford: *Physica B* 198 (1995) 33. This proof uses the rectangular (binned) representation of potentials. A general proof for continuous potentials also can be given. 11)
 - 10) In the general case the rhs of eq. (18) is $A^2+B^2+C^2+D^2$. 11)
 - 11) N.F. Berk: unpublished.
 - 12) For real potentials and in the absence of bound states, $t(k_z)$ ---but not necessarily $r(k_z)$ ---generally satisfies a logarithmic dispersion relation. For potentials with bound states, the logarithmic dispersion must be augmented by a sum of pole terms, which entails knowledge of the location and residues of the poles of $t(k_z)$ in the upper half-plane.
 - 13) H. Fiedeldey, R. Lipperheide, H. Leeb, and S.A. Sofianos: *Physics Letters A* 170 (1992) 347.
 - 14) W.L. Clinton: *Phys. Rev. B* 48 (1993) 1. Clinton discusses conditions under which $r(k_z)$ may satisfy a logarithmic dispersion relation.
 - 15) F.W. Byron, Jr. and R.W. Fuller: *Mathematics of Classical and Quantum Physics* (Addison-Wesley, Reading, 1969).
 - 16) Marchenko⁹⁾ presents a rigorous derivation of the Povzner-Levitan kernel appropriate for potentials having half-line or compact support.
 - 17) B.N. Zakhariev and A.A. Suzko: *Direct and Inverse Problems* (Springer-Verlag, New York, 1990).
 - 18) T.M. Roberts: *Physica B* 173 (1991) 157.
 - 19) e.g., B.W. Koenig, S. Krueger, W.J. Orts, C.F. Majkrzak, N.F. Berk, J.V. Silverton, and K. Gawrisch: *Langmuir*, in press.